

---

# Meta-Learning a Real-Time Tabular AutoML Method For Small Data

---

**Noah Hollmann \***

University of Freiburg &  
Berlin Institute of Health  
Charité University Medicine Berlin  
noah.hollmann@charite.de

**Samuel Müller \***

University of Freiburg  
muellesa@cs.uni-freiburg.de

**Katharina Eggensperger**

University of Freiburg  
eggenspk@cs.uni-freiburg.de

**Frank Hutter**

University of Freiburg &  
Bosch Center for Artificial Intelligence  
fh@cs.uni-freiburg.de

## Abstract

We present TabPFN, an AutoML method that is competitive with the state of the art on small tabular datasets while being over  $1\,000\times$  faster. Our method is very simple: it is fully entailed in the weights of a single neural network, and a single forward pass directly yields predictions for a new dataset. Our AutoML method is meta-learned using the Transformer-based Prior-Data Fitted Network (PFN) architecture and approximates Bayesian inference with a prior that is based on assumptions of simplicity and causal structures. The prior contains a large space of structural causal models and Bayesian neural networks with a bias for small architectures and thus low complexity. Furthermore, we extend the PFN approach to differentially calibrate the prior’s hyperparameters on real data. By doing so, we separate our abstract prior assumptions from their heuristic calibration on real data. Afterwards, the calibrated hyperparameters are fixed and TabPFN can be applied to any new tabular dataset at the push of a button. Finally, on 30 datasets from the OpenML-CC18 suite we show that our method outperforms boosted trees and performs on par with complex state-of-the-art AutoML systems with predictions produced in less than a second. We provide all our code and our final trained TabPFN in the supplementary materials.

## 1 Introduction

Machine learning (ML) algorithms for tabular data are essential for many real-world applications in areas like medicine, finance, research, predictive maintenance or sensor data modelling. While neural networks excel on many ML tasks, Gradient-Boosted Decision Trees (GBDT) still dominate the landscape of supervised ML for tabular data [13, 30], largely due to their short training time and robustness.

Hands-free Automated Machine Learning (AutoML) systems for tabular data have been shown to push the limits of ML even further [31, 15, 7]. However, to achieve this, AutoML systems automatically evaluate and combine a large set of different ML algorithms, thus requiring substantial resources and becoming increasingly complex. State-of-the-art AutoML tools combine several classifiers, various preprocessing tools, advanced hyperparameter optimization methods [9], meta-learning [11, 36] and

---

\*Equal contribution.

ensembling [8, 10, 21, 12, 7]. These stacked complexities can lead to system failures on the user side [7] that can be hard to understand.

AutoML systems are usually benchmarked for several hours, and in our experiments, an AutoML training took at least minutes. This makes applications such as instant classification in a spreadsheet infeasible. We propose a radical change to this pipeline that slashes the required time to *a single second* and simplifies the application to a neural network (NN) forward-pass, a stable and highly portable standard procedure that could even be run on handheld devices.

Our method builds on Prior-Data Fitted Networks (PFNs) [18], which meta-learn to approximate the posterior predictive distribution (PPD) for a prior over supervised learning problems that one can sample data from. Approximating the PPD implements prediction under Bayesian principles. PFNs work for any prior that we are able to sample data from. By doing so, a prediction algorithm can be meta-learned and complex prior assumptions can be encoded through sampling schemes. This fundamentally changes the way learning algorithms are designed. In the original PFN paper [18], PPD approximation with PFNs was, amongst other experiments, demonstrated on binary classification for very small, balanced tabular datasets with only up to 30 training examples and very few features. We build on this work to create a state-of-the-art model for tabular multi-class classification tasks that we evaluate on real-world loads of up to 1 000 training examples, 100 features and 10 classes.

We use a prior based on Bayesian Neural Networks (BNNs [20, 14]) and Structural Causal Models (SCMs [22, 24]) to model complex dependencies in tabular data. Our prior also takes ideas from Occam’s razor: simpler models with fewer variables have a higher likelihood. By assuming a causal structure and a notion of simplicity in our prior, the PFN performs Bayesian inference over a space of hypotheses that is modelled through a structural causal framework and weighted by simplicity.

Finally, since there are many decisions to be made when building a prior like this, we broadly hyperparameterize our prior, learn a single NN to support this broad prior and accept hyperparameters of the prior during inference time. We introduce a gradient-based methodology to tune these hyperparameters post hoc on real (meta-validation) datasets. This simplifies the development of PFN priors and reduces the number of models to be trained to one.

In this paper, we make the following contributions:

- We present a state-of-the-art AutoML method for small, tabular datasets that yields more than  $1000\times$  speedup over previous methods.
- We design a Bayesian PFN prior on the space of Structural Causal Models, taking into account millions of models during training.
- We introduce differentiable hyperparameter tuning for PFNs, which allows broad and flexible priors that can be refined on a set of real (meta-validation) datasets with gradient descent.

## 2 Prior-Data Fitted Networks

PFNs leverage large-scale ML techniques to enable fast approximation of a large set of PPDs [18]. PFNs are NNs that accept a variable length training set  $D_{train} = \{(x_1, y_1), \dots, (x_n, y_n)\}$  of input vectors and output labels and a query vector  $x$  as input and return an estimate of the PPD  $p(y|x, D_{train})$ . They rely on a Transformer that encodes each data point in  $D_{train}$  as a token [33]. There are two distinct phases in which we use PFNs: the *(meta-)training* phase and the *inference* phase.

**Meta-Training** During meta-training the PFN  $q_\theta$  is trained to make probabilistic predictions for a held-out example  $(x, y) \in D$  based on the rest of a dataset  $D_{train}$ , where  $D$  is an artificial dataset drawn from a pre-defined prior  $p(D)$ . The PFN is trained to minimize the following expectation over sampled datasets:

$$\mathcal{L}_{PFN} = \mathbb{E}_{\{(x,y), D_{train}\} \sim p(D)} [q_\theta(y|x, D_{train})] \quad (1)$$

For efficiency reasons, we use more than one hold-out example per dataset  $D$  in practice. We detail the full training setup in Algorithm 1 in the appendix. Crucially, this *(meta-)training* phase is performed only once for a given prior  $p(D)$ , learning to do *inference* on any dataset in a single forward pass.

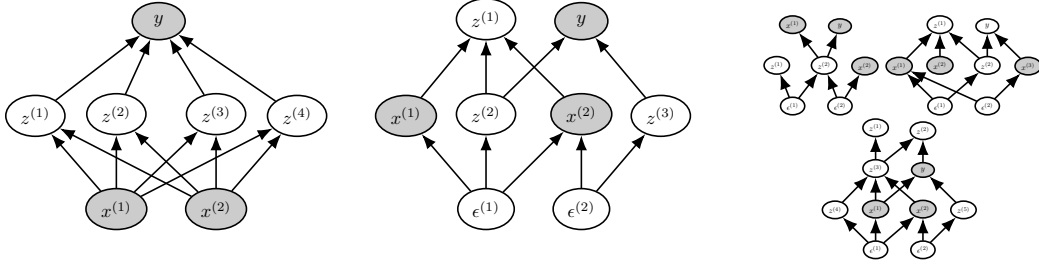


Figure 1: Left: A BNN. Center: A SCM. Right: Samples from a prior over SCM architectures; PFNs consider a distribution over different model architectures at once. Center and Right: The inputs  $x$  are mapped to the output  $y$  (grey nodes) with independent noise variables  $\epsilon$  added to all nodes.

**Inference** During the inference phase PFNs approximate the PPD, to make predictions for an unseen real dataset. The entire dataset and held-out samples are fed as inputs to the PFN and predictions are made per held-out sample. Thus, training and prediction is done in one single forward pass (similar to prediction with Gaussian Processes), which is different from the standard pipeline in ML, where we train and then evaluate in two distinct phases.

### 3 A Prior for Tabular Data

The performance of our method crucially depends on the specification of a suitable prior, as the PFN approximates the PPD for this prior. In the Bayesian framework for supervised learning, the prior defines a space of hypotheses  $\Phi$  on the relationship of the inputs to the output labels. In this work we consider a hypothesis space over Structural Causal Models (SCMs) and Bayesian Neural Networks (BNNs). TabPFN learns to approximate integration over the space of hypotheses  $\Phi$  (i.e., SCMs and BNNs), where the weight of a hypothesis is determined by its prior probability (which we chose to generally align with simplicity, see Section 3.1) and the likelihood of the observations given this hypothesis. Training a PFN only requires to specify a prior sampling scheme  $p(D) = \mathbb{E}_{\phi \sim p(\phi)}[p(D|\phi)]$  and generate samples with  $\phi \sim p(\phi)$  and then  $D \sim p(D|\phi)$ .

This simple setup enables ensembling different kinds of priors and hyperparameters: all we need to do is to define our prior over the hypotheses  $\Phi$  as  $p(\phi) = \mathbb{E}_{a \sim p(a)}[p(\phi|a)]$ . Here,  $a$  could, for example, be a random variable defining the architecture of a BNN (as done by Müller et al. [18]). In Section 3.1, we extend this approach to a mixture of a BNN and a structural causal prior, each of which entails a mixture of architectures and hyperparameters by themselves.

In the remainder of this section, we discuss the components of our prior. We describe additional refinements to our prior to reflect tabular data better in Appendix D.2.

#### 3.1 Simplicity and Causal Mechanisms

**Simplicity** We base our priors on a notion of simplicity, such as stated by Occam’s Razor or the Speed Prior [27]. When considering competing hypotheses, the simpler one, e.g. the one requiring less parameters, is to be preferred. Work in cognitive science has uncovered this preference for simple explanations in human thinking as well [35]. A notion of simplicity, however, depends on choosing a language to define simplicity in. In the following, we introduce prior models based on SCMs and BNNs, in which simplicity materializes as graphs with few nodes and parameters. Thus, our model prefers hypotheses based on simple SCMs or BNNs during inference capturing the notion of simple explanations.

**BNN Prior** For the first part of our prior, we use the BNN prior as introduced by Müller et al. [18]. To sample a dataset from this prior, we first sample a NN architecture and its weights. Then, for each data point in the to-be-generated dataset, we sample an input  $x \sim \mathcal{N}(\mathbf{0}, \mathbf{I})$ , feed it through the network and use the output  $y$  as a target (see Figure 1)<sup>2</sup>. This is a more general setup than in standard BNNs, as the posterior also considers a distribution over architectures with a bias towards simple

<sup>2</sup>We note that, while tabular data is not always normalized, we apply z-normalization to the columns.

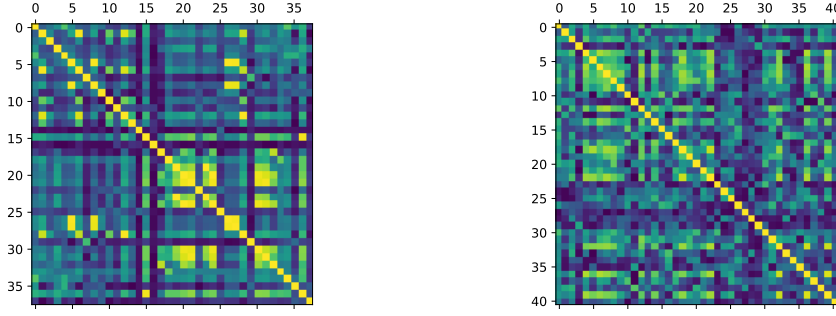


Figure 2: Feature Correlation matrices, brighter colors indicate higher correlation. Left: Real world data from the “PC4 Software defect prediction” dataset. Right: Synthetic data generated by a causal prior with blockwise sampling as explained in Appendix D.2.

architectures, not only the standard distribution over a fixed architecture’s weights. Details of this method can be found in Müller et al. [18].

**Structural Causal Prior** It has been demonstrated that causal knowledge can facilitate various ML tasks, including semi-supervised learning and transfer learning [29]. Here, we extend the BNN prior above to represent a subclass of SCMs [22, 24] as visualized in Figure 1. An SCM over a set of random variables  $Z = \{z_1, \dots, z_m\}$  is defined as a set of structural assignments (called mechanisms), where each variable  $z_i$  is defined by a deterministic function

$$z_i = f_i(Z_{\text{PA}_{\mathcal{G}}(i)}, \epsilon_i), \quad (2)$$

where  $\text{PA}_{\mathcal{G}}(i)$  is the set of parents of  $z_i$  (its direct causes) in an underlying DAG  $\mathcal{G}$  and  $f_i$  is a (potentially non-linear) deterministic function. Variables in  $Z$  can be observed (endogenous), i.e., be part of the set of features or labels, or unobserved (exogenous). We make the common assumption that  $\mathcal{G}$  does not contain cycles. Thus, relationships can be represented by a directed acyclic graph (DAG), called the causal graph induced by  $\mathcal{G}$ , with edges  $E$  pointing from causes to effects.

We use a prior for simplicity over SCMs by preferring a low number of connections and nodes in the SCM’s DAG. We use a subfamily of SCMs as described in the following sampling scheme. There are no theoretical constraints on the subfamily of SCMs other than that we can sample from it. We chose this framework since (1) tabular data sets often exhibit causal relationships between columns, and (2) causal mechanisms have been shown to be a strong prior in human reasoning [34, 35].

While we do not perform causal inference, we use a prior over SCMs, to yield a PFN approximating a PPD that is compatible with causal relationships in the data and exhibits strong real-world performance. This is not easy to do with traditional Bayesian methods, i.e. Variational Inference and Markov Chain Monte Carlo, as the hypothesis space is a distribution over many graphs. Thus, a representation of an infinitely large space of hypotheses and their uncertainty would need to be modelled by these methods. While Annadani et al. [1] extends this representation to the space of discrete DAGs it is limited to few subfamilies of SCMs and the computational complexity is high.

PFNs provably approximate Bayesian inference, effectively reasoning over the full space of hypotheses, i.e. graphs of SCMs, and their respective weights in a single forward pass.

**The Sampling Algorithm** We instantiate a subfamily of DAGs that can be efficiently sampled from by starting with an MLP-architecture and dropping weights from it. That is, to sample a dataset with  $k$  features and  $n$  samples from our prior we perform the following steps for each dataset:

- (1) We sample the number of MLP layers  $l \sim p(l)$  and nodes  $h \sim p(h)$  and sample a graph  $\mathcal{G}(Z, E)$  structured like an  $l$ -layered MLP with hidden size  $h$ .
- (2) We sample weights for each Edge  $E_{ij}$  as  $W_{i,j} \sim p_w(\cdot)$ .
- (3) We drop a random set of edges  $e \in E$  to yield a random DAG.
- (4) We sample a set of  $k$  feature nodes  $N_x$  and a label node  $N_y$  from the the nodes  $Z$ .
- (5) We sample the noise distributions  $p(\epsilon) \sim p(p(\epsilon))$  from a meta-distribution. This yields an SCM, with all  $f_i$ ’s instantiated as random affine mappings followed by an activation. Each  $z_i$  corresponds to a sparsely connected neuron in the MLP.

With the above parameters fixed, we perform the following steps for each member of the dataset:

- (1) We sample noise variables  $\epsilon_i$  from their specific distributions.
- (2) We compute the value of all  $z \in Z$  with  $z_i = a((\sum_{j \in \text{PA}_{\mathcal{G}(i)}} E_{ij} z_j) + \epsilon_i)$ .
- (3) We read off the values at the feature nodes  $N_x$  and the output node  $N_y$  and return them.

We sample one activation function  $a$  per dataset from  $\{ReLU, Tanh, Identity\}$  [19]. The sampling scheme for the number of layers  $p(l)$  and nodes  $p(h)$  is designed to follow a log-normal distributions, the dropout rate follows a beta distribution and  $p(p(\epsilon))$  samples normal distributions with normally distributed mean and standard deviation. The resulting features and targets are correlated through the generating DAG structure. This leads to conditionally dependent features, dependent through forward and backward causation, i.e. targets might be a cause or an effect of features. In Figure 2 we exemplify the resulting correlations between features and compare them to a real-world dataset and in Figure 7 in the appendix we showcase scatter plots of the features of this prior for different classes.

### 3.2 Multi-class Prediction

So far, the described priors apply only to regression tasks, i.e. return scalar labels. In this work we tackle tabular classification and, thus, we need to transform our regression labels to classification labels. We perform the following steps to map the continuous labels  $\hat{y}$  to discrete labels:

- (1) We sample the number of classes  $N_c \sim p(N_c)$ , a hyperparameter.
- (2) We sample the class distribution, by uniformly  $[0, 1]$  sampling  $N_c - 1$  quantile bounds  $B_c \sim p(B_c|N_c)$  that define  $N_c$  quantile ranges  $R$ . For example for  $N_c = 2$  the quantile bound  $B_c = \{0.5\}$  would define two quantile ranges  $\{[0.0, 0.5], [0.5, 1.0]\}$  and thus balanced binary labels.
- (3) We map each scalar label  $\hat{y}_i$  to the discrete quantile range label  $y_i \leftarrow \sum_j B_j < \text{rank}(\hat{y}_i)/n$ , where  $\text{rank}$  maps  $\hat{y}_i$  to its rank in  $\hat{y}$ .
- (4) With probability  $p_s$ , a hyperparameter, we shuffle the labelling of classes, that is, we remove the ordering of class labels wrt. the quantile range.

Defining the prior sampling scheme laid out in the previous sections, a mix of regression priors (Section 3.1) combined with a way to create classification dataset samples from them (Section 3.2), is all that is needed to train a PFN to perform Bayesian predictions on tabular data, i.e. make predictions for held-out examples of unseen tabular datasets.

## 4 Differentiable Tuning of the Prior's Hyperparameters

A very diverse prior, like the one described above, comes with a lot of hyperparameters for its many sub-components. Specifically, our prior has 35 hyperparameters (for full details see Appendix F). Tuning this large number of hyperparameters with the standard black-box methods, e.g., random search or Bayesian optimization, would be very expensive, due to the curse of dimensionality [17].

Instead, we tune the prior's hyperparameters with backpropagation. To be able to do this, when training the PFN, we teach it how to predict with different prior hyperparameters; and then, after training on prior samples, we use a meta-validation set of actual datasets to choose the final hyperparameters.

In Figure 3, we detail the training. For the generation of each training dataset we first sample  $\psi$ , the hyperparameters of the prior. Then, we sample a dataset from the prior given  $\psi$  and fit the PFN to each dataset prepending an embedding of  $\psi$  as an input token. Thus information about the hyperparameters underlying the prior distribution of each dataset is passed to the network as well. The objective becomes minimizing the KL-Divergence to the true posterior for hyperparameters sampled from a fixed distribution  $p(\psi)$ .

The new objective, thus, is an expectation over cross-entropy terms for many different PPDs:

$$\mathbb{E}_{\psi \sim p(\psi), (x, D_{train}) \sim p(x, D_{train}|\psi)} [\text{CE}(p(\cdot|x, D_{train}, \psi), q_\theta(\cdot|x, D_{train}, \psi))]. \quad (3)$$

This objective minimizes the KL-Divergence between the true posterior and the approximation. Therefore, we approximate the true posterior across hyperparameter settings in  $p(\psi)$  and our method can be seen as a "conditional PFN" that computes the PPD for a prior with given hyperparameters. We show this with a simple derivation in Appendix E.1, similar to the derivations of Müller et al. [18]. Additionally, we combine this approach with the hyperparameter ensembling approach described in the introduction of Section 3: Hyperparameters are not fixed values, but are defined as distributions

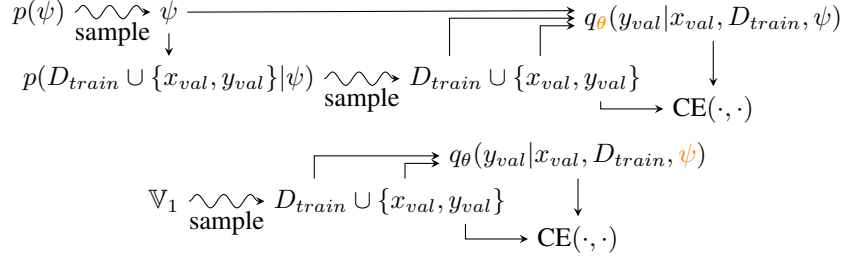


Figure 3: A visualization of the meta-training in the top and hyperparameter tuning setup in the bottom. We sample hyperparameters (HPs) along with artificial datasets and optimize the HP embedding  $\theta$ , while we sample real validation datasets during hyperparameter tuning and optimize the style  $\psi$ .

over values in the prior, e.g., categorical hyperparameters are specified as the probability of the categories occurring and are sampled for each dataset.

To allow the PFN to accept  $\psi$ , we simply prepend a token, a learned linear projection of  $\psi$  to the embedding size of the underlying Transformer. After training our (conditional) PFN, we have an approximation of the PPD for all  $\psi$  in the support of  $p(\psi)$ . In our experimental setup, we choose one global hyperparameter setting  $\psi^*$  that is then used for all experiments with new (meta-test) datasets. Since we want to choose  $\psi^*$  such that the resulting posterior models tabular datasets well, we created a set of representative meta-validation datasets  $\mathbb{V}$  (detailed in Table 7). We randomly split  $\mathbb{V}$  into a set of 90 datasets  $\mathbb{V}_1$  and 60 datasets  $\mathbb{V}_2$ . Next we optimize  $\psi$  using gradient descent on the loss for  $\mathbb{V}_1$ . That is, we initialize  $\psi \sim p(\psi)$  at random and perform gradient descent on  $\mathbb{V}_1$  to minimize the cross-entropy on the evaluation examples in all the meta-validation datasets in  $\mathbb{V}_1$  given  $\psi$ . We visualize this in Figure 3. We use  $\mathbb{V}_2$  for early stopping in the differentiable hyperparameter tuning procedure. We also use  $\mathbb{V}_2$  to choose one final  $\psi^*$  out of  $N$  independent optimizations from different initializations. We outline this approach in Algorithm 2 in the appendix.

**Relation to Prior Work** Passing hyperparameters during inference is used in the Style Transformer which uses this information to influence the style of the language at inference time [6]. Our setup, on the other hand, chooses prior hyperparameters and, different from Dai et al. [6], we perform a gradient-based optimization of  $\psi$  after training the (conditional) PFN in a meta-validation phase, but before seeing any meta-test datasets. Zhang et al. [39] optimize some input tokens in a gradient-based fashion to do prompt tuning, these tokens however do not represent hyperparameters in any sense, but instead words. MacKay et al. [16] follows a similar approach, but while that method requires intricate adaptations of the network architecture to condition network weights on hyperparameters, our method is customized to our specific setup, allowing it to be far simpler and more efficient.

**Ablation on Tuning Gaussian Process Hyperparameters** To demonstrate the efficiency of differentiable hyperparameter tuning, we show that it can successfully recover the right hyperparameters in an example task. We trained a PFN on a simple Gaussian Process (GP) prior with an RBF kernel, where we sample the output scale and length scale uniformly from  $[0, 10]$ , and the noise from  $[0.01, 0.5]$ . We group the  $y$  values for each meta-train dataset sampled from the prior into the top- and bottom-half and treat this as a binary classification problem.

After training, we consider a GP prior with fixed hyperparameters as validation distribution (representing both  $\mathbb{V}_1$  and  $\mathbb{V}_2$  from above) and analyze whether we can recover its hyperparameters with differentiable hyperparameter tuning. We generate samples  $S$  from Gaussian Processes using the true hyperparameters  $\hat{\psi}$  indicated by the dashed blue line. We report the results in Figure 4. The cross-entropy of the PFN with different values for each hyperparameter in  $\psi$  chosen over its whole range (keeping the others at their optimal value), is given by the solid blue line. As expected, for all hyperparameters, when the model is provided with the correct value it performs best. We also performed differentiable hyperparameter tuning, as described above, on all hyperparameters, resulting in the values for each hyperparameter marked by the red lines and recovering the hyperparameter values of our validation distribution almost exactly.

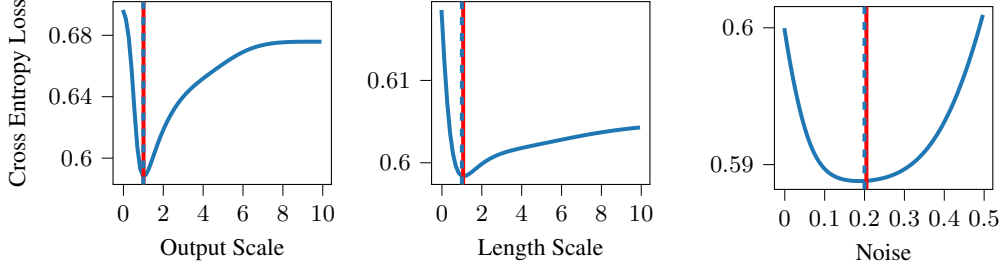


Figure 4: Estimating the hyperparameters of a Gaussian Process. The solid blue indicates the loss of a PFN given the hyperparameter indicated on the x-axis. The dashed (a) blue and (b) red lines indicate the (a) true and (b) estimated hyperparameters.

## 5 Experiments

Now, we turn to an empirical analysis of our method for actual classification tasks. We empirically compare our method against commonly used ML and AutoML methods for tabular classification tasks with small data and conduct an ablation analysis to show the importance of our design decisions.

### 5.1 Evaluation on Tabular AutoML Tasks

First, we empirically analyze the predictive performance of our method and compare against state-of-the-art methods for tabular AutoML. We briefly describe our experimental setup before we turn to discussing the results and provide further details in Appendix G.

**Datasets** We use three disjoint sets of datasets in our experiments, all focussing on tabular classification tasks with small data. As *meta-test* datasets, we used a set of 30 datasets from the curated open-source OpenML-CC18 benchmark suite [3], and as *meta-validation* datasets  $\mathbb{V}_1$  and  $\mathbb{V}_2$  we used 150 datasets from OpenML.org [32] that we randomly split into two sets of size 90 ( $\mathbb{V}_1$ ) and 60 ( $\mathbb{V}_2$ ). We made sure that none of the datasets in  $\mathbb{V}$  are contained in the *meta-test* datasets. We give a full description of all datasets and how we collected them in Appendix G.3.

**Baselines** We compare against five standard ML methods and two state-of-the-art AutoML systems for tabular data. As ML models we considered two simple and fast baselines, *K-nearest-neighbors* (KNNs) and *Logistic Regression* (LogReg), additionally we considered Gaussian Processes (GPs) [26] and two popular tree-based boosting methods, *XGBoost* [5] and *CatBoost* [25]. For each ML model, we used 5-fold cross-validation to evaluate randomly drawn configurations until a given budget was exhausted or 1 000 configurations were evaluated (for the search spaces, see Appendix G.2). We then refit the configuration with the lowest ROC AUC OVO error on the whole training set. Where necessary, we imputed missing values with the mean, one-hot encoded categorical inputs and normalized features. As more complex but also potentially powerful baselines, we chose two AutoML systems: *AutoGluon* [7] which combines ML models including neural networks and tree-based models into a stacked ensemble and *Auto-sklearn 2.0* [10, 12] which uses Bayesian Optimization and combines the evaluated models into a weighted ensemble.<sup>3</sup>

**TabPFN** We follow the architecture used in the original PFN paper [18], which uses a Transformer Encoder [33] with a specific attention mask and without positional encodings. We meta-train the TabPFN once on the prior described in Section 3 for 20 hours on 8 GPUs, yielding a meta-learned algorithm that can be used for any new dataset. We note that while this step is expensive it is done offline, in advance and only once for all, as part of the algorithm development. We applied the following steps to apply the TabPFN: (1) We train a PFN on the prior as in Section 3; (2) We differentially tune the prior's hyperparameters as in Section 4; (3) Similar to modern AutoML

<sup>3</sup>Auto-sklearn 2.0 optimizes ROC AUC for binary classification and cross-entropy for multi-class classification (as multi-class ROC AUC is not implemented). AutoGluon optimizes cross-entropy on all datasets since this produced better performance and we thus picked the stronger baseline (and report the other results in Appendix G).

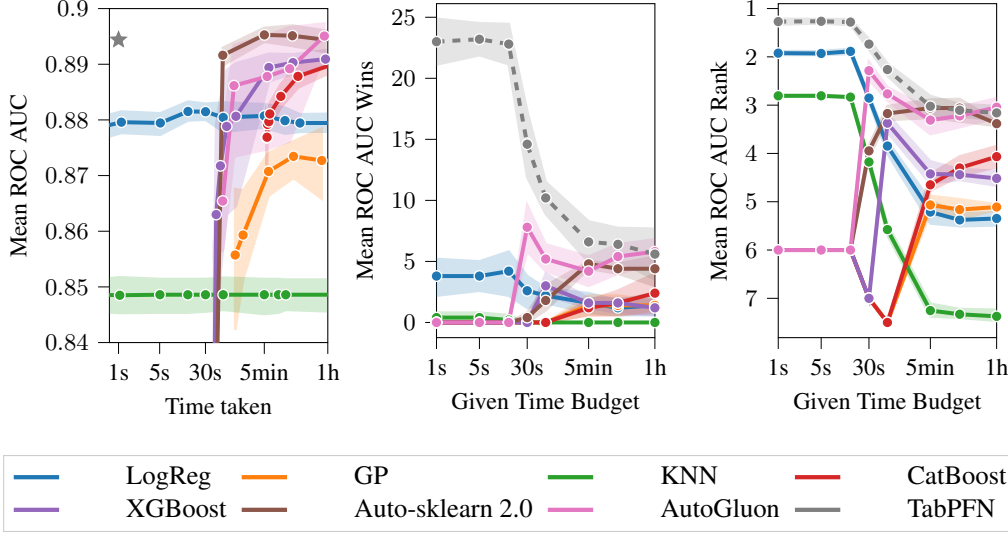


Figure 5: ROC AUC performance over time. We report mean ROC, mean wins and rank along with the 95% confidence interval across 5 repetitions for different time budgets. Results that take more than 100% more time budget than requested are not plotted in rank and wins plot.

systems, we ensemble 10 instantiations of our TabPFN with randomly permuted feature dimensions and labels<sup>4</sup> and vary preprocessing using a robust or power scaler [37]. During inference we also apply z-normalization. Further details and hyperparameters used can be found in Appendix F.

**Evaluation Protocol** For each dataset and method, we evaluated 5 repetitions, each with a different random seed and a different train- and test split (all methods used the same split given a seed). To aggregate results across datasets, we report the ROC AUC (ROC AUC one-vs-one (OVO) for multi-class classification) average, ranks and wins including the 95% confidence interval and compare to the performance of the baselines with a budget of [30, 60, 300, 900, 3600] seconds<sup>5</sup>. Our TabPFN is run 10 times with the above permutations, taking 1.0 seconds for the full benchmark on a GPU (or 13.2 seconds on a single CPU).

**Results** We present the achieved AUC ROC as a function of budget in Figure 5, demonstrating that TabPFN is dramatically ( $1\,000\times$ ) faster than all the other methods while yielding competitive or better predictions: it makes predictions within a single second (on GPU) that tie with the performance of the best competitors (the AutoML systems) after training one hour, and that dominate the performance achieved by competitors in 5 minutes. Unsurprisingly, the simple baselines (LogReg, KNN) already yield results with a small budget but perform worst overall for larger budgets. Boosted tree-based methods (XGBoost, CatBoost) perform better, but are clearly outperformed by the two state-of-the-art AutoML systems. The AutoML systems are the best-performing baselines. Given enough budget ( $\geq 15$  minutes) they achieve competitive performance with our TabPFN (which uses a fixed time budget of 1 second in all comparisons). We provide further detailed results, including results per dataset and other metrics in Appendix G.

## 5.2 Ablation and Generalization Study

**Tuning the Hyperparameters of the Tabular Prior** Figure 6 shows the optimization curves during differentiable hyperparameter tuning. When we compare model results before and after differentiable hyperparameter tuning, we can see clear improvements in cross-entropy.

<sup>4</sup>Otherwise, the network has biases we do not want, e.g. preferring label 0 in case of uncertainty; this is resolved by permuting labels. We note that this arises from the prior implementation in this work and could be solved in the prior as well.

<sup>5</sup>When comparing methods to each other for a given time budget in Figure 5, we drop methods that take more than 200% of the time budget requested; some methods also do not use their full budget.



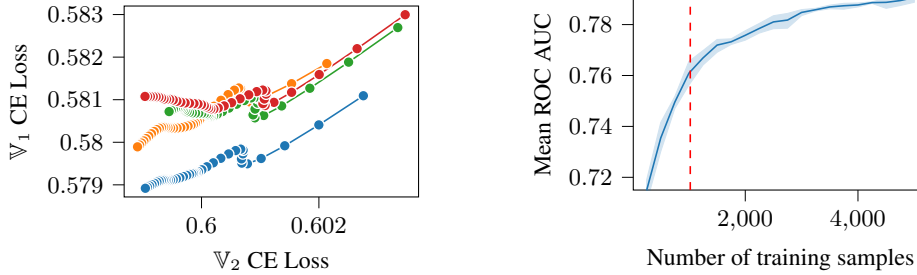


Figure 6: Left: Differentiable Hyperparameter Tuning loss curves of both sets of validation datasets  $\mathbb{V}_1$  and  $\mathbb{V}_2$ : We perform multiple (different colors) gradient-descent optimizations of  $\phi$  on  $\mathbb{V}_1$  from different random initializations and choose the best performer on  $\mathbb{V}_2$ . The best configuration is used on test data in our models. Right: Extrapolation performance of our TabPFN to dataset sizes never seen during training. Maximum number of samples during training was 1024 (dashed red line).

**Prior Ablations** We perform ablation experiments for a prior based solely on BNNs, SCMs and a mix of both using a hyperparameter to control the sampling likelihood for either. The PFNs for each prior are fitted using less compute than in our final experiments, thus their scores generally are slightly worse. For each, we perform differentiable hyperparameter tuning as described in Section 4 and report results in Table 1. We can see that the choice of prior is crucial. The BNN prior, which is similar to the one used in Müller et al. [18], provides clearly diminished performance compared to the priors based on causal models. Additionally, we can see that mixing BNN and SCM prior does not seem to make big difference on our test set compared to a pure SCM prior.

	BNN	SCM	SCM + BNN
Mean CE	0.811 $\pm$ 0.009	<b>0.771</b> $\pm$ 0.006	0.776 $\pm$ 0.009
Mean ROC AUC	0.865 $\pm$ 0.007	0.881 $\pm$ 0.002	<b>0.883</b> $\pm$ 0.003

Table 1: An evaluation of the impact of the prior mixing on the final performance. Our final model was trained in the *SCM + BNN* setting, see Section 3 for details on the priors.

**Model Generalization** The Transformer-based PFN architecture accepts a dataset of any length as input. When training this architecture however, the generated datasets are limited to a maximum size of 1024. Here, we create a collection of datasets from the OpenML AutoML benchmark with up to 10 000 samples and evaluate on up to 5 000 training samples. That is a 5-fold increase as compared to the dataset sizes seen during meta-training of the PFN. Surprisingly we find that our models generalize to sizes that were never seen during training, as can be seen in Figure 6. That is Average ROC AUC significantly improves when more training data is provided. The list of datasets used and experiment details can be found in Appendix G.

## 6 Conclusions & Future Work

We have shown how a single Transformer, the TabPFN, can be trained to do the work of a full AutoML framework for tabular data and can yield predictions in 1 second that are competitive with the performance that the best available AutoML frameworks achieve in 1 hour. This result is likely to disrupt the field of data science, since it allows for real-time predictions. It also presents a turning point for the computational expense of AutoML, allowing for sustainable, green, AutoML.

TabPFN still has important limitations (detailed in Appendix A) that motivate a multitude of exciting follow-ups regarding (1) regression tasks, (2) scaling up to large datasets, (3) inclusion of classical ML model classes in the prior, (4) ensembling to continue making improvements given more time; (5) quantification of aleatoric and epistemic uncertainty, (6) studies of interpretability and robustness; (7) generalizations to non-tabular data; and (8) dataset-dependent choices of the prior. The almost instant state-of-the-art predictions of TabPFN are also likely to give rise to (9) novel exploratory data analysis methods, (10) novel feature engineering methods and (11) novel active learning methods.

## References

- [1] Y. Annadani, J. Rothfuss, A. Lacoste, N. Scherrer, A. Goyal, Y. Bengio, and S. Bauer. Variational causal networks: Approximate Bayesian inference over causal structures. *arXiv:2106.07635 [cs.LG]*, 2021. 4
- [2] I. Beltagy, M. Peters, and A. Cohan. Longformer: The long-document transformer. *arXiv:2004.05150 [cs.CL]*, 2020. 13
- [3] B. Bischl, G. Casalicchio, M. Feurer, P. Gijsbers, F. Hutter, M. Lang, R. Mantovani, J. van Rijn, and J. Vanschoren. OpenML benchmarking suites. In J. Vanschoren, S. Yeung, and M. Xenochristou, editors, *Proceedings of the Neural Information Processing Systems Track on Datasets and Benchmarks*. Curran Associates, 2021. 7, 17
- [4] V. Borisov, T. Leemann, K. Seßler, J. Haug, M. Pawelczyk, and G. Kasneci. Deep neural networks and tabular data: A survey. *arXiv:2110.01889 [cs.LG]*, 2021. 14
- [5] T. Chen, S. Kornblith, K. Swersky, M. Norouzi, and G. Hinton. Big self-supervised models are strong semi-supervised learners. *arXiv:2006.10029*, 2020. 7
- [6] N. Dai, J. Liang, X. Qiu, and X. Huang. Style transformer: Unpaired text style transfer without disentangled latent representation. In *Proceedings of the 57th Annual Meeting of the Association for Computational Linguistics (ACL'19)*, pages 5997–6007, 2019. 6
- [7] N. Erickson, J. Mueller, A. Shirkovand, H. Zhang, P. Larroy, M. Li, and A. Smola. Autogluon-tabular: Robust and accurate automl for structured data. *arXiv:2003.06505 [cs.LG]*, 2020. 1, 2, 7
- [8] H. Escalante, M. Montes, and E. Sucar. Particle Swarm Model Selection. *Journal of Machine Learning Research*, 10:405–440, 2009. 2
- [9] S. Falkner, A. Klein, and F. Hutter. BOHB: Robust and efficient hyperparameter optimization at scale. In J. Dy and A. Krause, editors, *Proceedings of the 35th International Conference on Machine Learning (ICML'18)*, volume 80, pages 1437–1446. Proceedings of Machine Learning Research, 2018. 1
- [10] M. Feurer, A. Klein, K. Eggensperger, J. Springenberg, M. Blum, and F. Hutter. Efficient and robust automated machine learning. In C. Cortes, N. Lawrence, D. Lee, M. Sugiyama, and R. Garnett, editors, *Proceedings of the 28th International Conference on Advances in Neural Information Processing Systems (NeurIPS'15)*, pages 2962–2970. Curran Associates, 2015. 2, 7
- [11] M. Feurer, J. Springenberg, and F. Hutter. Initializing Bayesian hyperparameter optimization via meta-learning. In B. Bonet and S. Koenig, editors, *Proceedings of the Twenty-ninth National Conference on Artificial Intelligence (AAAI'15)*, pages 1128–1135. AAAI Press, 2015. 1
- [12] M. Feurer, K. Eggensperger, S. Falkner, M. Lindauer, and F. Hutter. Auto-sklearn 2.0: Hands-free AutoML via meta-learning. *arXiv:2007.04074 [cs.LG]*, 2021. 2, 7
- [13] J. Friedman. Greedy function approximation: a gradient boosting machine. *Annals of statistics*, pages 1189–1232, 2001. 1
- [14] Y. Gal. *Uncertainty in Deep Learning*. PhD thesis, University of Cambridge, 2016. 2
- [15] F. Hutter, L. Kotthoff, and J. Vanschoren, editors. *Automated Machine Learning: Methods, Systems, Challenges*. Springer, 2019. Available for free at <http://automl.org/book>. 1
- [16] M. MacKay, P. Vicol, J. Lorraine, D. Duvenaud, and R. Grosse. Self-tuning networks: Bilevel optimization of hyperparameters using structured best-response functions. *arXiv:1903.03088 [cs.LG]*, 2019. 6
- [17] D. Maclaurin, D. Duvenaud, and R. Adams. Gradient-based Hyperparameter Optimization through Reversible Learning. In F. Bach and D. Blei, editors, *Proceedings of the 32nd International Conference on Machine Learning (ICML'15)*, volume 37, pages 2113–2122. Omnipress, 2015. 5

- [18] Samuel Müller, Noah Hollmann, Sebastian Pineda Arango, Josif Grabocka, and Frank Hutter. Transformers can do bayesian inference. In *International Conference on Learning Representations*, 2022. URL <https://openreview.net/forum?id=KSugKcbNf9>. 2, 3, 4, 5, 7, 9, 13, 15
- [19] V. Nair and G. Hinton. Rectified linear units improve restricted Boltzmann machines. In J. Fürnkranz and T. Joachims, editors, *Proceedings of the 27th International Conference on Machine Learning (ICML'10)*. Omnipress, 2010. 5
- [20] R. Neal. *Bayesian Learning for Neural Networks*. Lecture Notes in Computer Science. Springer, 1996. 2
- [21] R. Olson, N. Bartley, R. Urbanowicz, and J. Moore. Evaluation of a Tree-based Pipeline Optimization Tool for Automating Data Science. In T. Friedrich, editor, *Proceedings of the Genetic and Evolutionary Computation Conference (GECCO'16)*, pages 485–492. ACM, 2016. 2
- [22] J. Pearl. *Causality*. Cambridge University Press, 2 edition, 2009. 2, 4
- [23] F. Pedregosa, G. Varoquaux, A. Gramfort, V. Michel, B. Thirion, O. Grisel, M. Blondel, P. Prettenhofer, R. Weiss, V. Dubourg, J. Vanderplas, A. Passos, D. Cournapeau, M. Brucher, M. Perrot, and E. Duchesnay. Scikit-learn: Machine learning in Python. *Journal of Machine Learning Research*, 12:2825–2830, 2011. 17
- [24] J. Peters, D. Janzing, and B. Schölkopf. *Elements of causal inference: foundations and learning algorithms*. The MIT Press, 2017. 2, 4
- [25] L. Prokhorenkova, G. Gusev, A. Vorobev, A. Dorogush, and A. Gulin. CatBoost: unbiased boosting with categorical features. In S. Bengio, H. Wallach, H. Larochelle, K. Grauman, N. Cesa-Bianchi, and R. Garnett, editors, *Proceedings of the 31st International Conference on Advances in Neural Information Processing Systems (NeurIPS'18)*. Curran Associates, 2018. 7
- [26] C. Rasmussen and C. Williams. *Gaussian Processes for Machine Learning*. The MIT Press, 2006. 7
- [27] J. Schmidhuber. The speed prior: A new simplicity measure yielding near-optimal computable predictions. In J. Kivinen and R. Sloan, editors, *Computational Learning Theory*, pages 216–228. Springer, 2002. 3
- [28] R. Schwartz, J. Dodge, N. Smith, and Etzioni. Green AI. *Communications of the ACM*, 63(12): 54–63, 2020. 13
- [29] B. Schölkopf, D. Janzing, J. Peters, E. Sgouritsa, K. Zhang, and J. Mooij. On causal and anticausal learning. In J. Langford and J. Pineau, editors, *Proceedings of the 29th International Conference on Machine Learning (ICML'12)*, pages 459–466. Omnipress, 2012. 4
- [30] R. Shwartz-Ziv and A. Armon. Tabular data: Deep learning is not all you need. *Information Fusion*, 81:84–90, 2022. 1, 17, 18
- [31] C. Thornton, F. Hutter, H. Hoos, and K. Leyton-Brown. Auto-WEKA: combined selection and hyperparameter optimization of classification algorithms. In I. Dhillon, Y. Koren, R. Ghani, T. Senator, P. Bradley, R. Parekh, J. He, R. Grossman, and R. Uthrusamy, editors, *The 19th ACM SIGKDD International Conference on Knowledge Discovery and Data Mining (KDD'13)*, pages 847–855. ACM Press, 2013. 1
- [32] J. Vanschoren, J. van Rijn, B. Bischl, and L. Torgo. OpenML: Networked science in machine learning. *SIGKDD Explorations*, 15(2):49–60, 2014. 7, 17
- [33] A. Vaswani, N. Shazeer, N. Parmar, J. Uszkoreit, L. Jones, A. Gomez, L. Kaiser, and I. Polosukhin. Attention is all you need. In I. Guyon, U. von Luxburg, S. Bengio, H. Wallach, R. Fergus, S. Vishwanathan, and R. Garnett, editors, *Proceedings of the 30th International Conference on Advances in Neural Information Processing Systems (NeurIPS'17)*. Curran Associates, Inc., 2017. 2, 7

- [34] M. Waldmann and Y. Hagmayer. Causal reasoning. *The Oxford handbook of cognitive psychology*, pages 733—752, 2013. 4
- [35] Z. Wojtowicz and S. DeDeo. From probability to consilience: How explanatory values implement bayesian reasoning. *Trends in Cognitive Sciences*, 24(12):981–993, 2020. 3, 4
- [36] C. Yang, J. Akimoto, D. Kim, and M. Udell. OBOE: Collaborative filtering for AutoML model selection. In A. Teredesai, V. Kumar, Y. Li, R. Rosales, E. Terzi, and G. Karypis, editors, *Proceedings of the 25th ACM SIGKDD International Conference on Knowledge Discovery & Data Mining, KDD’19*, pages 1173–1183. ACM Press, 2019. 1
- [37] I. Yeo and R. Johnson. A new family of power transformations to improve normality or symmetry. *Biometrika*, 87(4):954–959, 2000. 8, 14
- [38] M. Zaheer, G. Guruganesh, K. Dubey, J. Ainslie, C. Alberti, S. Ontanon, P. Pham, A. Ravula, Q. Wang Qifan, L. Yang, and A. Amr. Big bird: Transformers for longer sequences. In H. Larochelle, M. Ranzato, R. Hadsell, M.-F. Balcan, and H. Lin, editors, *Proceedings of the 33rd International Conference on Advances in Neural Information Processing Systems (NeurIPS’20)*, pages 17283–17297. Curran Associates, 2020. 13
- [39] N. Zhang, L. Li, X. Chen, S. Deng, Z. Bi, C. Tan, F. Huang, and H. Chen. Differentiable prompt makes pre-trained language models better few-shot learners. In *Proceedings of the International Conference on Learning Representations (ICLR’22)*, 2022. Published online: iclr.cc. 6

## A Limitations

The runtime and memory usage of the Transformer-based PFN architecture used in this work scales quadratically with the number of inputs, i.e. training samples passed. Thus, inference on larger sequences ( $> 100\,000$ ) is hard on current consumer GPUs. A growing number of methods seek to tackle this issue and report similar performances while scaling linearly with the number of inputs [38, 2]. These methods can be integrated in the PFN architecture and thus into TabPFN. Furthermore, in our experiments we limit the number of features to 100 and the number of classes to 10 as described in Section 5. While this choice is flexible, our fitted TabPFN can not work with datasets that go beyond these limits.

## B Societal Implications

In terms of broader societal impact of this work, we do not see any foreseeable strongly negative impacts. However, this paper could positively impact the carbon footprint and accessibility of learning algorithms. The computations required for machine learning research have been doubling every few months, resulting in a large carbon footprint [28]. Moreover, the financial cost of the computations can make it difficult for academics, students, and researchers to apply these methods. The decreased computational time shown by TabPFN translates to gains in CO2 emissions and cost, making it available to an audience that does not have access to larger scale computing.

## C Details of Prior-Data Fitted Network Algorithm

Algorithm 1 describes the training method proposed by Müller et al. [18] for PFNs.

---

**Algorithm 1:** Meta-Training of a PFN [18]

---

**Input** : A prior distribution over datasets  $p(D)$ , from which samples can be drawn and the number of samples  $K$  to draw

**Output** : A model  $q_\theta$  that will approximate the PPD

Initialize the neural network  $q_\theta$ ;

**for**  $j \leftarrow 1$  **to**  $K$  **do**

    Sample  $D \cup \{(x_i, y_i)\}_{i=1}^m \sim p(D)$ ;

    Compute stochastic loss approximation  $\bar{\ell}_\theta = \sum_{i=1}^m (-\log q_\theta(y_i|x_i, D))$ ;

    Update parameters  $\theta$  with stochastic gradient descent on  $\nabla_\theta \bar{\ell}_\theta$ ;

**end**

---

## D Details of the TabPFN Prior

In this section, we describe additional methods included in our prior. First, we describe mixing in Gaussian Process (GP) priors as another way to diversify the hypotheses approximated by TabPFN. Next, we describe refinements to our prior for the usage on tabular data. Figure 7 visualizes exemplary samples generated by an SCM prior.

### D.1 GP Prior

Tabular datasets are heterogenous in the kind of data described, i.e. the hypotheses space induced by BNN and SCM priors might not be appropriate for all datasets. As described in Section 3, the Bayesian formulation our TabPFN also allows for mixing different kinds of priors, generated by a distinct model. In addition to mixing BNN and SCM priors we also mix in a prior based on Gaussian Processes (GPs). As described in the work of Müller et al. [18] we approximate an RBF Kernel with varying hyperparameters (outputscale, lengthscale and noise) and apply the multiclass labelling described in Section 3.2. Our experiments showed no significant improvement with adding a GP prior to the mixture of BNN and SCM priors. However, this approach points out an area of future work in which distinct kinds of prior models such as CNNs could be added to the mix of priors.

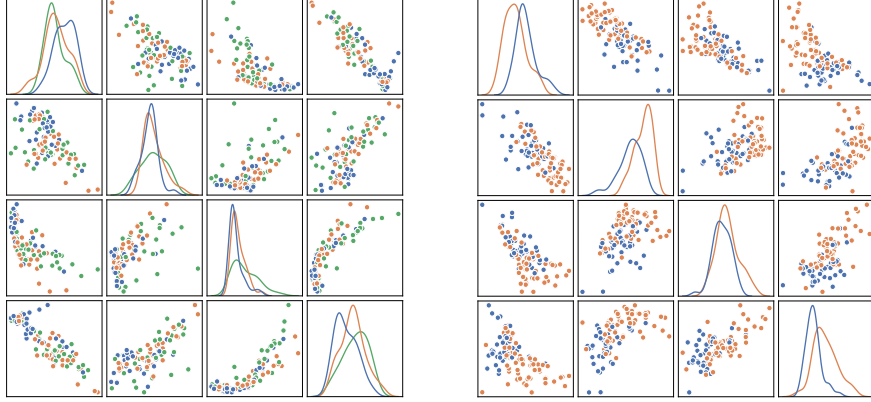


Figure 7: 100 samples generated by our causal tabular prior with 4 features. Each point represents a sample with colors indicating the class label. Each plot off the diagonal indicates the values of two features. The diagonal shows histograms of each class and feature. In a causal prior, features are generated from a common generating graph and so share the same generating processes. This can be seen as features tend to be correlated and seem to be simple transformations of each other.

## D.2 Tabular Data Refinement

Tabular datasets comprise a range of peculiarities, e.g. feature types can be numerical, ordinal, or categorical and feature values can be missing leading to sparse features. We seek to reflect these peculiarities in the design of our prior as described in the following sections.

### D.2.1 Preprocessing

During meta-training input data is normalized to zero mean and variance and we apply the same step when evaluating on real data. Since tabular data frequently contains exponentially scaled data, which is not might not be present during meta-training, we apply robust and power scaling during inference [37]. Thus, during inference on real tabular datasets the features more closely match those seen during meta-training. This preprocessing time is taken into account when reporting the inference time of our method.

### D.2.2 Correlated Features

Feature correlation in tabular data varies between datasets and ranges from independent to highly correlated. This poses problems to classical deep learning methods [4]. When considering a large space of structural causal models correlated features of varying degrees naturally arise in our priors. Furthermore, in real world tabular data the ordering of features is often unstructured, however adjacent features are often more highly correlated than others. We use "Blockwise feature sampling" to also reflect the correlation structure between ordered features. Our generation method of structural causal models naturally provides a way to do this. The first step in generating our SCMs is generating a unidirectional layered network structure in which nodes in one layer can only receive inputs from the preceding layer. Thus, features in one layer tend to be higher correlated. We use this by sampling adjacent nodes in the layered network structure in blocks and using these ordered blocks in our set of features.

### D.2.3 Nan Handling

In order to model missing values in our prior, we introduce missing values probabilistically during prior training. For each dataset, we sample a binary decision variable  $M$ , indicating whether it will contain missing features and next sample a fraction  $f_m$  of missing values. If  $M$  is positive, we drop out a fraction  $f_m$  of feature values uniformly at random. We introduce a binary missing value mask,

indicating the positions of missing values, and pass it to our model alongside the feature embedding. We append this mask during meta-training on synthetic data and inference on actual datasets.

#### D.2.4 Categorical Features

Tabular data often includes not only numeric features, but also discrete categorical ones. A categorical feature can be ordered, i.e. the categories represent binned degrees of some underlying variable, or shuffled. We introduce categorical features, by picking a random fraction  $p_{cat}$  (a hyperparameter) of categorical features per dataset. Analogous to transforming numeric class labels to discrete multiclass labels, we convert dense features to discrete ones. Also analogous to multiclass labels, we pick a shuffling fraction of categorical features  $p_{scat}$  where we reshuffle categories. For details see 3.2. Our experiments regarding categorical features however showed no significant improvement. Finding more appropriate ways of handling categorical features could be a line of future research.

### E Details for Differentiable Hyperparameter Tuning

#### E.1 Derivation of Claims for Differentiable Hyperparameter Tuning

We can discern three distinct claims in Section 4.

**i) Minimizing Equation 3 is equivalent to minimizing the KL-Divergence.** This is a simple standard proof regarding the connection between cross-entropy and KL-Divergence. One variant is noted in Müller et al. [18] in Corollary 1.1.

**ii) Our objective is Equation 3.** In the following we derive that Equation 3 actually is the loss we minimize, we broadly follow Insight 1 of Müller et al. [18]. This derivation starts with  $L_{PFN}$  as defined in Equation 1, which we extend with hyperparameters as described in Section 4 and derive the loss as described in Equation 3

$$\mathbb{E}_{\psi \sim p(\psi)} \left[ \mathbb{E}_{(y, x, D_{train}) \sim p(y, x, D_{train} | \psi)} [-\log q_{\theta}(y | x, D_{train}, \psi)] \right] \quad (4)$$

$$\mathbb{E}_{\psi \sim p(\psi)} \left[ \mathbb{E}_{(x, D_{train}) \sim p(x, D_{train} | \psi)} \left[ \mathbb{E}_{y \sim p(y | x, D_{train}, \psi)} [-\log q_{\theta}(y | x, D_{train}, \psi)] \right] \right] \quad (5)$$

$$\mathbb{E}_{\psi \sim p(\psi)} \left[ \mathbb{E}_{(x, D_{train}) \sim p(x, D_{train} | \psi)} [CE(p(y | x, D_{train}, \psi), q_{\theta}(y | x, D_{train}, \psi))] \right] \quad (6)$$

$$= \mathbb{E}_{\psi \sim p(\psi), (x, D_{train}) \sim p(x, D_{train} | \psi)} [CE(p(\cdot | x, D_{train}, \psi), q_{\theta}(\cdot | x, D_{train}, \psi))] . \quad (7)$$

For most hyperparameters we simply use a uniform distribution as  $p(\psi)$ , thus we can view this objective as minimizing the average distance for all considered hyperparameters  $\psi$ .

**iii) We approximate the true posterior across hyperparameters.** This is a trivial insight, given i) and ii). We know that our loss is equivalent to an expectation over KL-Divergences, up to a constant. Thus, minimizing our objective will lead to closer solutions in terms of the expectation over KL-Divergences. Assuming there is a  $\theta$  with  $p = q_{\theta}$  we can make this claim tighter. We know that the KL-Divergence between two distributions  $p_1$  and  $p_2$  is zero iff  $p_1 = p_2$ . Thus, our objective is minimal iff  $p = q_{\theta}$ , as shown by Müller et al. [18] in Corollary 1.2. This in turn implies equality for all hyperparameters  $\psi$ .

#### E.2 Softmax temperature calibration

In addition to differentially tuning the prior's hyperparameters, as described in Section 4, we also introduce a softmax temperature factor, that is differentially tuned on our meta-train and meta-validation dataset alongside the hyperparameters  $\psi$ . That is when decoding the logits produced by our TabPFN to probabilities we perform the following calculation:

$$p_{TabPFN}(logit, t) = \frac{\exp(x_i/t)}{\sum_j \exp(x_j/t)},$$

---

**Algorithm 2:** Differentiable Hyperparameter Tuning

---

**Input** : Two sets of validation datasets  $\mathbb{V}_1$  and  $\mathbb{V}_2$  and a PFN  $q(y|x, D, \psi)$ .

**Output** : Final hyperparameters to use the model with  $\psi^*$ .

Initialize the neural network  $q_\theta$ ;

**for**  $d \leftarrow 1$  **to**  $\text{num\_draws}$  **do**

    Sample initial  $\psi_d^{(0)} \sim p(\psi)$ ;

**for**  $s \leftarrow 1$  **to**  $\text{num\_steps}$  **do**

$g \leftarrow 0$ ;

**foreach**  $D_{\text{train}}, \{(x_{\text{val}}^{(1)}, y_{\text{val}}^{(1)}), \dots, (x_{\text{val}}^{(m)}, y_{\text{val}}^{(m)})\} \in \mathbb{V}_1$  **do**

$l \leftarrow \sum_i \text{CE}(q(\cdot|x_{\text{val}}^{(i)}, D_{\text{train}}, \psi_d^{(s-1)}), y_{\text{val}}^{(i)})$ ;

$g \leftarrow g + \frac{dl}{d\psi_d}$ ;

**end**

        Take optimizer step with aggregated gradients  $\psi_d^{(s)} \leftarrow \text{Adam}(\psi_d^{(s-1)}, g)$ ;

**end**

**end**

Finally, choose best performer on  $\mathbb{V}_2$  from all  $\psi_d^{(s)}$  and return it as  $\psi^*$ .

---

where  $\text{logit}_i$  is the logit probability for class  $i$  and  $t$  is the temperature factor. During differentiable hyperparameter tuning we also propagate the cross entropy loss on the meta-train datasets to the factor  $t$  and use early stopping on the meta-validation datasets for the best combination of  $t$  and prior hyperparameters  $\psi$ .

## F Setup of our method

### F.1 Transformer Hyperparameters

While, most of our hyperparameters are tuned with differentiable hyperparameter tuning, the hyperparameters of our transformer architecture and training are not part of the prior and can thus not be tuned in the same way. We considered only PFN Transformers with 12 layers, embeddings size 512, hidden size 1024 in feed-forward layers, and 4-head attention. For each training we tested a set of 3 learning rates,  $\{.001, .0003, .0001\}$ , and used the one with the lowest final training loss.

### F.2 TabPFN Training

We trained our final model for 18 000 steps with a batch size of 512 datasets. That is, during training our PFN sees 9 216 000 datasets. This training takes 20 hours on 8 GPUs (Nvidia RTX 2080 Ti). Each dataset had a fixed size of 1024 and we split it into training and validation uniformly at random. We generally saw that learning curves tended to flatten after around 10 million datasets and were generally very noisy. Likely, this is because our prior generates a wide variety of different datasets.

### F.3 Prior Hyperparameters

The hyperparameters of our prior were tuned using differentiable hyperparameter tuning. For the distributions of the hyperparameters tuned with differentiable hyperparameter tuning see Table 2. Hyperparameters that specify sampling distributions other than uniform are made up of one or more underlying uniform distributions. Choice HPs are made up of one hyperparameter per choice, except for the first choice. Beta distributions are made up of two parameters  $\alpha$  and  $\beta$ . Truncated Normals are made up of a mean and a standard deviation. The *Min* value is added to the HP to give a lower bound. If Rounding is enabled, Hps will be rounded to the next value after sampling. The model receives the values of each underlying parameter making up these distributions during differentiable hyperparameter tuning.



Table 2: Overview of our priors hyperparameters optimized using differentiable hyperparameter tuning.

	Sampling distribution $p(\psi)$	Minimum	Maximum		
GP sampling likelihood	Uniform	0.5	8.0		
		Min $\alpha$ and $\beta$	Max $\alpha$ and $\beta$	Scale HP	
MLP weight dropout	Beta	0.1	5.0	0.9	
Choices					
Sample SCM	Choice	[True, False]			
Share Noise mean for nodes	Choice	[True, False]			
Sample y from last MLP layer	Choice	[True, False]			
MLP Activation Functions	Choice	[Tanh, ReLU, ELU]			
MLP Activation Functions	Choice	, Identity, Threshold]			
Blockwise Dropout	Choice	[True, False]			
Keep SCM feature order	Choice	[True, False]			
Sample features blockwise	Choice	[True, False]			
GP noise	Choice	[1e-05, 0.0001, 0.01]			
		Max Mean	Min Mean	Round HP	Min
MLP #layers	Trunc. Normal	6	1	True	2
MLP #hidden nodes per layer	Trunc. Normal	130	5	True	4
Gaussian Noise Std.	Trunc. Normal	0.3	0.0001	False	0.0
MLP Weights Std.	Trunc. Normal	10.0	0.01	False	0.0
SCM #nodes at layer 1	Trunc. Normal	12	1	True	1
GP outputscale	Trunc. Normal	10.0	0.00001	False	0
GP lengthscale	Trunc. Normal	10.0	0.00001	False	0

## G Details for Tabular Experiments

Here we provide additional details for the experiments conducted in Section 5 in the main paper.

### G.1 Hardware Setup

All evaluations, including the baselines, ran on a compute cluster equipped with Intel(R) Xeon(R) Gold 6242 CPU @ 2.80GHz using 1 CPU with up to 6GB RAM. For evaluation using our TabPFN, we additionally use a RTX 2080 Ti.

### G.2 Baselines

We provide the search space used to tune our baselines in Table 3. For *CatBoost* and *XGBoost*, we used the same ranges as Shwartz-Ziv and Armon [30] with the following exceptions: For *CatBoost* we removed the hyperparameter `max_depth` since it is not in documentation, for *CatBoost* and *XGBoost*, we set the range for `n_estimators` to be in  $[100, 4000]$ . The search spaces for the KNN, GP and Logistic Regression baselines were designed from scratch and we used the respective implementation from *scikit-learn* [23]. For Catboost and AutoSklearn we pass the position of categorical features to the classifier (AutoGluon automatically detects categorical feature columns). We normalize inputs for Logistic Regression, GP and KNN to the range  $[0, 1]$  using MinMax Scaling.

### G.3 Used Datasets

To construct and evaluate our method, we use three disjoint sets of datasets. Our test-set (see Table 6), a subset of the OpenML-CC18 benchmark suite [3] and a meta-set (see Table 7 and 8), which we collected from OpenML.org [32]. These are licensed under the BSD 3-Clause license.

For the test-set, we considered all datasets in the OpenML-CC18 benchmark suite with less than 2 000 samples, 100 features or 10 classes, which leaves us with 30 datasets that represent small, tabular datasets. For the meta-set, we considered all datasets on OpenML.org and applied the following

Table 3: Hyperparameter spaces for baselines. Adapted from Shwartz-Ziv and Armon [30].

baseline	name	type	log	range
LogReg	penalty	cat	(11, 12, none)	-
	max_iter	int	[50, 500]	-
	fit_intercept	cat	(True, False)	-
	C	float	$[e^{-5}, 5]$	-
KNN	n_neighbors	int	[1, 16]	-
GP	params_y_scale	float	[0.05, 5.0]	yes
	params_length_scale	float	[0.1, 1.0]	yes
CatBoost	learning_rate	float	$[e^{-5}, 1]$	yes
	random_strength	int	[1, 20]	-
	l2_leaf_reg	float	[1, 10]	yes
	bagging_temperature	float	[0, 1.0]	yes
	leaf_estimation_iterations	int	[1, 20]	-
	iterations	int	[100, 4000]	-
XGBoost	learning_rate	float	$[e^{-7}, 1]$	yes
	max_depth	int	[1, 10]	-
	subsample	float	[0.2, 1]	-
	colsample_bytree	float	[0.2, 1]	-
	colsample_bylevel	float	[0.2, 1]	-
	min_child_weight	float	$[e^{-16}, e^5]$	yes
	alpha	float	$[e^{-16}, e^2]$	yes
	lambda	float	$[e^{-16}, e^2]$	yes
	gamma	float	$[e^{-16}, e^2]$	yes
	n_estimators	int	[100, 4000]	-

filtering procedure: We dropped all datasets that are in the test-set (and manually checked for overlaps) and all datasets with more than 1 000 samples, 100 features or 10 classes. Furthermore, we manually dropped FOREX (since it is a time series dataset) and artificially created datasets, such as autoUniv and Friedman datasets. The remaining meta-set then contains of 150 datasets.

#### G.4 Additional Results

In addition to the results in the main paper in Section 5.1, we report a wide range of performance values in Table 4. We show quantitative results for comparing all methods when given up to 15min time. We see that our model is competitive with strong AutoML baselines while requiring a fraction of that time. Furthermore, we report ROC AUC performance over time, similarly to Figure 5, except that AutoGluon optimizes for ROC AUC. While the mean rank and number of wins remains similar, the average AUC ROC performance decreases in our experiments, due to failure to train Catboost models on 2 datasets (MiceProtein, mfeat-zernike).

#### G.5 Model Generalization

For testing the TabPFN performance on longer sequences, as described in Section 6, we used a set of datasets from the OpenML AutoML Benchmark that contain at least 10 000 samples. The list of datasets used can be found in Table 5. Datasets with more than 100 features are limited to the first 100 features. When more than 10 classes are contained in the datasets, samples with any but the first 10 classes are discarded.

## H Code

Our code alongside notebooks to reproduce our experiments and pretrained models are available at <https://github.com/noahho/TabPFN>.

Table 4: ROC AUC OVO results on the small OpenML-CC18 for 15 minutes requested time per dataset and per split. If available, all baselines are given ROC AUC optimization as an objective, others optimize CE. Overall each method got a time budget of 37.5 hours, but not all methods used the full budget.

	KNN	LogReg	GP	CatBoost	XGBoost	Auto-sklearn2.0	AutoGluon	TabPFN
balance-scale	0.88	0.962	0.983	0.92	0.992	<b>0.997</b>	0.992	0.996
mfeat-fourier	0.97	0.976	0.952	0.981	0.98	<b>0.983</b>	<b>0.983</b>	0.982
breast-w	0.984	<b>0.994</b>	0.992	0.992	0.991	<b>0.994</b>	<b>0.994</b>	0.993
mfeat-karhunen	0.994	0.995	0.99	<b>0.999</b>	0.998	0.998	<b>0.999</b>	0.998
mfeat-morph...	0.951	0.964	0.959	0.963	0.961	0.966	<b>0.969</b>	0.968
mfeat-zernike	0.976	0.979	0.937	0.972	0.97	0.981	<b>0.989</b>	0.983
cmc	0.634	0.675	0.673	0.712	0.727	<b>0.738</b>	0.732	0.726
credit-approval	0.914	0.92	0.921	<b>0.941</b>	0.937	0.938	<b>0.941</b>	0.932
credit-g	0.726	0.758	0.774	0.783	0.785	0.789	<b>0.795</b>	0.79
diabetes	0.806	0.84	0.832	<b>0.842</b>	0.837	0.839	0.838	<b>0.842</b>
tic-tac-toe	0.986	0.995	0.998	0.999	0.997	0.998	<b>1</b>	0.966
vehicle	0.881	0.933	0.901	0.93	0.927	0.946	0.942	<b>0.958</b>
eucalyptus	0.798	0.885	0.828	0.895	0.902	0.919	0.919	<b>0.927</b>
analcata_a...	<b>1</b>	<b>1</b>	0.983	<b>1</b>	<b>1</b>	<b>1</b>	<b>1</b>	<b>1</b>
analcata_dmft	0.543	0.56	0.574	0.544	0.577	<b>0.582</b>	0.568	0.58
pc4	0.822	0.891	0.899	0.941	0.928	0.936	<b>0.942</b>	0.939
pc3	0.753	0.781	0.795	0.825	0.83	0.829	0.824	<b>0.834</b>
kc2	0.79	0.823	0.828	0.812	0.814	0.831	0.823	<b>0.836</b>
pc1	0.785	0.821	0.824	0.854	0.843	0.856	0.861	<b>0.877</b>
banknote-auth...	0.999	<b>1</b>	<b>1</b>	<b>1</b>	<b>1</b>	<b>1</b>	<b>1</b>	<b>1</b>
blood-transfus...	0.708	0.749	0.757	0.751	0.734	0.749	0.739	<b>0.759</b>
ilpd	0.646	0.721	0.663	0.719	0.719	0.722	0.73	<b>0.736</b>
qsar-biodeg	0.892	0.92	0.922	0.923	0.922	0.928	0.926	<b>0.933</b>
wdbc	0.991	0.995	0.995	0.994	0.994	<b>0.996</b>	<b>0.996</b>	<b>0.996</b>
cylinder-bands	0.781	0.813	0.839	0.875	<b>0.883</b>	0.867	0.726	0.846
dresses-sales	0.557	0.6	<b>0.624</b>	0.575	0.58	0.569	0.555	0.534
MiceProtein	0.997	0.998	<b>1</b>	<b>1</b>	<b>1</b>	<b>1</b>	<b>1</b>	<b>1</b>
car	0.924	0.98	0.885	0.995	0.993	<b>0.998</b>	0.997	0.997
steel-plates-fault	0.92	0.935	0.934	0.966	0.966	<b>0.969</b>	0.967	0.966
climate-model-...	0.849	0.931	<b>0.941</b>	0.933	0.922	0.937	0.93	0.939
Wins AUC OVO	0	0	2	0	1	5	5	<b>8</b>
Wins Acc.	0	3	1	2	1	4	6	<b>10</b>
Wins CE	0	0	1	0	2	1	<b>13</b>	11
Win/T/L AUC vs Us	2/0/28	3/0/27	3/1/26	7/1/22	5/0/25	11/1/18	13/1/16	0/0/0
Win/T/L Acc vs Us	2/0/28	6/0/24	4/1/25	10/0/20	7/0/23	11/0/19	11/0/19	0/0/0
Win/T/L CE vs Us	0/0/30	1/0/29	3/0/27	4/0/26	4/0/26	6/0/24	15/0/15	0/0/0
Mean AUC OVO	0.849±0.015	0.88±0.012	0.873±0.024	0.888±0.012	0.89±0.012	<b>0.895±0.0097</b>	0.889±0.022	0.894±0.0097
Mean Acc.	0.785±0.016	0.809±0.014	0.774±0.075	0.818±0.013	0.82±0.014	0.818±0.025	0.825±0.021	<b>0.826±0.011</b>
Mean CE	1.79±1.1	0.769±0.027	0.859±0.068	0.774±0.073	0.763±0.059	0.839±0.065	<b>0.72±0.019</b>	0.731±0.015
M. rank AUC OVO	7.53	5.28	5.55	4.22	4.72	<b>2.75</b>	3.13	2.82
Mean rank Acc.	6.78	4.98	5.67	4.22	4.53	4.08	2.97	<b>2.77</b>
Mean rank CE	7.17	5.17	5.77	4.52	4.7	4.77	<b>1.78</b>	2.13
Mean time (s)	<b>0.5</b>	60	941.1	1121	921.9	901.5	809.1	0.99 (GPU) 13.2 (CPU)

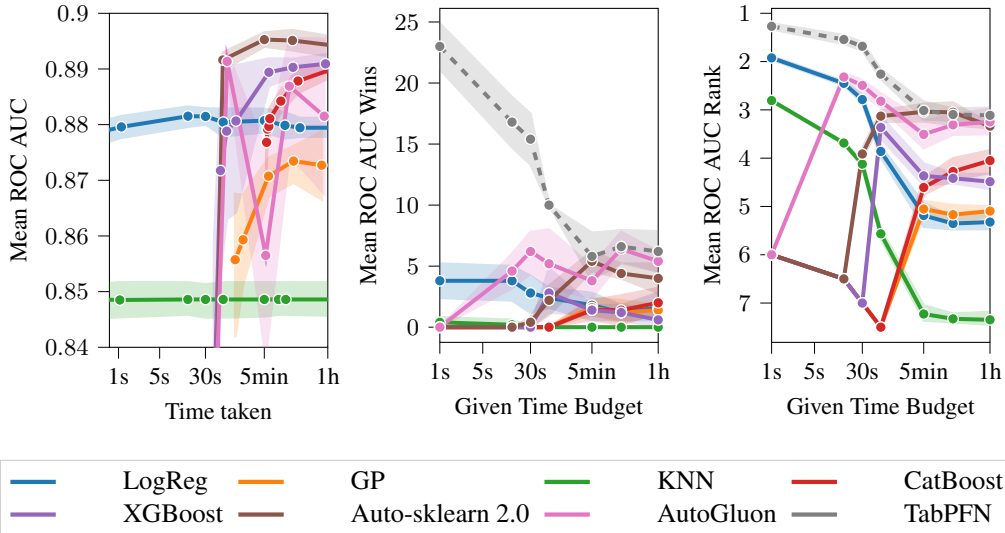


Figure 8: ROC AUC performance over time, as reported in Figure 5. But with Autoglun fails.

Table 5: Evaluation datasets for model generalization experiments.

Name	#Feat.	#Cat.	#Inst.	#Class.	#NaNs	Minor. Class Size	OpenML ID
KDDCup09_appetency	231	39	50000	2	8024152	890	1111
airlines	8	5	539383	2	0	240264	1169
bank-marketing	17	10	45211	2	0	5289	1461
nomao	119	30	34465	2	0	9844	1486
adult	15	9	48842	2	6465	11687	1590
covertype	55	45	581012	7	0	2747	1596
numera128.6	22	1	96320	2	0	47662	23517
connect-4	43	43	67557	3	0	6449	40668
jungle_chess_2pcs.	7	1	44819	3	0	4335	41027
APSFailure	171	1	76000	2	1078695	1375	41138
albert	79	53	425240	2	2734000	212620	41147
MiniBooNE	51	1	130064	2	0	36499	41150
guillermo	4297	1	20000	2	0	8003	41159
riccardo	4297	1	20000	2	0	5000	41161
volkert	181	1	58310	10	0	1361	41166
dionis	61	1	416188	355	0	878	41167
jannis	55	1	83733	4	0	1687	41168
helen	28	1	65196	100	0	111	41169

Table 6: Datasets used for the evaluation.

Name	#Feat.	#Cat.	#Inst.	#Class.	#NaNs	Minor. Class Size	OpenML ID
balance-scale	5	1	625	3	0	49	11
mfeat-fourier	77	1	2000	10	0	200	14
breast-w	10	1	699	2	16	241	15
mfeat-karhunen	65	1	2000	10	0	200	16
mfeat-morphological	7	1	2000	10	0	200	18
mfeat-zernike	48	1	2000	10	0	200	22
cmc	10	8	1473	3	0	333	23
credit-approval	16	10	690	2	67	307	29
credit-g	21	14	1000	2	0	300	31
diabetes	9	1	768	2	0	268	37
tic-tac-toe	10	10	958	2	0	332	50
vehicle	19	1	846	4	0	199	54
eucalyptus	20	6	736	5	448	105	188
anacatdata_auth...	71	1	841	4	0	55	458
anacatdata_dmft	5	5	797	6	0	123	469
pc4	38	1	1458	2	0	178	1049
pc3	38	1	1563	2	0	160	1050
kc2	22	1	522	2	0	107	1063
pc1	22	1	1109	2	0	77	1068
banknote-authenti...	5	1	1372	2	0	610	1462
blood-transfusion-...	5	1	748	2	0	178	1464
ilpd	11	2	583	2	0	167	1480
qsar-biodeg	42	1	1055	2	0	356	1494
wdbc	31	1	569	2	0	212	1510
cylinder-bands	40	22	540	2	999	228	6332
dresses-sales	13	12	500	2	835	210	23381
MiceProtein	82	5	1080	8	1396	105	40966
car	7	7	1728	4	0	65	40975
steel-plates-fault	28	1	1941	7	0	55	40982
climate-model-simu...	21	1	540	2	0	46	40994

Table 7: Meta-Datasets used for tuning the prior.

Name	#Feat.	#Cat.	#Inst.	#Class.	#NaNs	Minor. Class Size	OpenML ID
breast-cancer	10	10	286	2	9	85	13
colic	27	20	368	2	1927	136	25
dermatology	35	34	366	6	8	20	35
sonar	61	1	208	2	0	97	40
glass	10	1	214	6	0	9	41
haberman	4	2	306	2	0	81	43
tae	6	3	151	3	0	49	48
heart-c	14	8	303	2	7	138	49
heart-h	14	8	294	2	782	106	51
heart-statlog	14	1	270	2	0	120	53
hepatitis	20	14	155	2	167	32	55
vote	17	17	435	2	392	168	56
ionosphere	35	1	351	2	0	126	59
iris	5	1	150	3	0	50	61
wine	14	1	178	3	0	48	187
flags	29	27	194	8	0	4	285
hayes-roth	5	1	160	3	0	31	329
monks-problems-1	7	7	556	2	0	278	333
monks-problems-2	7	7	601	2	0	206	334
monks-problems-3	7	7	554	2	0	266	335
SPECT	23	23	267	2	0	55	336
SPECTF	45	1	349	2	0	95	337
grub-damage	9	7	155	4	0	19	338
synthetic_control	61	1	600	6	0	100	377
prnn_crabs	8	2	200	2	0	100	446
analcdata_lawsuit	5	2	264	2	0	19	450
irish	6	4	500	2	32	222	451
analcdata_broadwaymult	8	5	285	7	27	21	452
analcdata_reviewer	8	8	379	4	1418	54	460
backache	32	27	180	2	0	25	463
prnn_synth	3	1	250	2	0	125	464
schizo	15	3	340	2	834	163	466
profb	10	5	672	2	1200	224	470
analcdata_germangss	6	5	400	4	0	100	475
biomed	9	2	209	2	15	75	481
rmftsa_sleepdata	3	1	1024	4	0	94	679
diggle_table_a2	9	1	310	9	0	18	694
rmftsa_ladata	11	1	508	2	0	222	717
pwLinear	11	1	200	2	0	97	721
analcdata_vineyard	4	2	468	2	0	208	724
machine_cpu	7	1	209	2	0	56	733
pharynx	11	10	195	2	2	74	738
auto_price	16	2	159	2	0	54	745
servo	5	5	167	2	0	38	747
analcdata_wildcat	6	3	163	2	0	47	748
pm10	8	1	500	2	0	246	750
wisconsin	33	1	194	2	0	90	753
autoPrice	16	1	159	2	0	54	756
meta	22	3	528	2	504	54	757
analcdata_apnea3	4	3	450	2	0	55	764
analcdata_apnea2	4	3	475	2	0	64	765
analcdata_apnea1	4	3	475	2	0	61	767
disclosure_x_bias	4	1	662	2	0	317	774
bodyfat	15	1	252	2	0	124	778
cleveland	14	8	303	2	6	139	786
triazines	61	1	186	2	0	77	788
disclosure_x_tampered	4	1	662	2	0	327	795
cpu	8	2	209	2	0	53	796
cholesterol	14	8	303	2	6	137	798
chscase_funds	3	1	185	2	0	87	801
pbeseq	19	7	1945	2	1133	972	802
pbc	19	9	418	2	1239	188	810
rmftsa_ctoarrivals	3	2	264	2	0	101	811
chscase_vine2	3	1	468	2	0	212	814
chatfield_4	13	1	235	2	0	93	820
boston_corrected	21	4	506	2	0	223	825
sensory	12	12	576	2	0	239	826
disclosure_x_noise	4	1	662	2	0	329	827
autoMpg	8	4	398	2	6	189	831
kdd_el_nino-small	9	3	782	2	466	274	839
autoHorse	26	9	205	2	57	83	840
stock	10	1	950	2	0	462	841
breastTumor	10	9	286	2	9	120	844
analcdata_gsssexsurvey	10	6	159	2	6	35	852
boston	14	2	506	2	0	209	853
fishcatch	8	3	158	2	87	63	854
vinnie	3	1	380	2	0	185	860
mu284	11	1	284	2	0	142	880
no2	8	1	500	2	0	249	886
chscase_geyser1	3	1	222	2	0	88	895
chscase_census6	7	1	400	2	0	165	900
chscase_census5	8	1	400	2	0	193	906
chscase_census4	8	1	400	2	0	194	907
chscase_census3	8	1	400	2	0	192	908
chscase_census2	8	1	400	2	0	197	909
plasma_retinol	14	4	315	2	0	133	915
visualizing_galaxy	5	1	323	2	0	148	925
colleges_usnews	34	2	1302	2	7830	614	930

Table 8: Meta-Datasets used for tuning the prior (continued).

Name	#Feat.	#Cat.	#Inst.	#Class.	#NaNs	Minor. Class Size	OpenML ID
disclosure_z	4	1	662	2	0	314	931
socmob	6	5	1156	2	0	256	934
chscase_whale	9	1	228	2	20	111	939
water-treatment	37	16	527	2	542	80	940
lowbwt	10	8	189	2	0	90	941
arsenic-female-bladder	5	2	559	2	0	80	949
analcadata_halloffame	17	2	1340	2	20	125	966
analcadata_birthday	4	3	365	2	30	53	968
analcadata_draft	5	3	366	2	1	32	984
collins	23	3	500	2	0	80	987
prnn_fglass	10	1	214	2	0	76	996
jEdit_4.2_4.3	9	1	369	2	0	165	1048
mc2	40	1	161	2	0	52	1054
mw1	38	1	403	2	0	31	1071
jEdit_4.0_4.2	9	1	274	2	0	134	1073
PopularKids	11	5	478	3	0	90	1100
teachingAssistant	7	5	151	3	0	49	1115
lungcancer_GSE31210	24	3	226	2	0	35	1412
MegaWatt1	38	1	253	2	0	27	1442
PizzaCutter1	38	1	661	2	0	52	1443
PizzaCutter3	38	1	1043	2	0	127	1444
CostaMadre1	38	1	296	2	0	38	1446
CastMetal1	38	1	327	2	0	42	1447
KnuggetChase3	40	1	194	2	0	36	1448
PieChart1	38	1	705	2	0	61	1451
PieChart3	38	1	1077	2	0	134	1453
parkinsons	23	1	195	2	0	48	1488
planning-relax	13	1	182	2	0	52	1490
qualitative-bankruptcy	7	7	250	2	0	107	1495
sa-heart	10	2	462	2	0	160	1498
seeds	8	1	210	3	0	70	1499
thoracic-surgery	17	14	470	2	0	70	1506
user-knowledge	6	1	403	5	0	24	1508
wholesale-customers	9	2	440	2	0	142	1511
heart-long-beach	14	1	200	5	0	10	1512
robot-failures-lp5	91	1	164	5	0	21	1520
vertebra-column	7	1	310	3	0	60	1523
Smartphone-Based...	68	2	180	6	0	30	4153
breast-cancer-...	10	10	277	2	0	81	23499
LED-display-...	8	1	500	10	0	37	40496
GAMETES_Epistasis...	21	21	1600	2	0	800	40646
calendarDOW	33	21	399	5	0	44	40663
corral	7	7	160	2	0	70	40669
mofn-3-7-10	11	11	1324	2	0	292	40680
thyroid-new	6	1	215	3	0	30	40682
solar-flare	13	13	315	5	0	21	40686
threeOf9	10	10	512	2	0	238	40690
xd6	10	10	973	2	0	322	40693
tokyo1	45	3	959	2	0	346	40705
parity5_plus_5	11	11	1124	2	0	557	40706
cleve	14	9	303	2	0	138	40710
cleveland-nominal	8	8	303	5	0	13	40711
Australian	15	9	690	2	0	307	40981
DiabeticMellitus	98	1	281	2	2	99	41430
conference_attendance	7	7	246	2	0	31	41538
CPMP-2015-...	23	1	527	4	0	78	41919
TuningSVMs	81	1	156	2	0	54	41976
regime_alimentaire	20	17	202	2	17	41	42172
iris-example	5	1	150	3	0	50	42261
Touch2	11	1	265	8	0	27	42544
penguins	7	3	344	3	18	68	42585
titanic	8	5	891	2	689	342	42638